Colloids and Surfaces B: Biointerfaces 76 (2010) 32–37

Contents lists available at ScienceDirect

Colloids and Surfaces B: Biointerfaces

journal homepage: www.elsevier.com/locate/colsurfb

Studies on interaction of colloidal Ag nanoparticles with Bovine Serum Albumin (BSA)

Aswathy Ravindran[a], Anupam Singh[a], Ashok M. Raichur[b], N. Chandrasekaran[a], Amitava Mukherjee[a,*]

[a] Nano-biomedicine Research Group, School of Biosciences and Technology, VIT University, Vellore-632014, India
[b] Department of Materials Engineering, Indian Institute of Science, Bangalore, India

ARTICLE INFO

Article history:
Received 15 April 2009
Received in revised form 7 October 2009
Accepted 7 October 2009
Available online 7 November 2009

Keywords:
Biocompatibility
Silver nanoparticles
BSA
UV–vis spectra
Blue shift
Adsorption isotherm

ABSTRACT

Biofunctionalization of noble metal nanoparticles like Ag, Au is essential to obtain biocompatibility for specific biomedical applications. Silver nanoparticles are being increasingly used in bio-sensing applications owing to excellent optoelectronic properties. Among the serum albumins, the most abundant proteins in plasma, a wide range of physiological functions of Bovine Serum Albumin (BSA) has made it a model system for biofunctionalization. In absence of adequate prior reports, this study aims to investigate the interaction between silver nanoparticles and BSA. The interaction of BSA [0.05–0.85% concentrations] with Ag nanoparticles [50 ppm concentration] in aqueous dispersion was studied through UV–vis spectral changes, morphological and surface structural changes. At pH 7, which is more than the isoelectric point of BSA, a decrease in absorbance at plasmon peak of uninteracted nanoparticles (425 nm) was noted till 0.45% BSA, beyond that a blue shift towards 410 nm was observed. The blue shift may be attributed to enhanced electron density on the particle surfaces. Increasing pH to 12 enhanced the blue shift further to 400 nm. The conformational changes in BSA at alkaline pH ranges and consequent hydrophobic interactions also played an important role. The equilibrium adsorption data fitted better to Freundlich isotherm compared to Langmuir curve. The X-ray diffraction study revealed complete coverage of Ag nanoparticles by BSA. The scanning electron microscopic study of the interacted nanoparticles was also carried out to decipher morphological changes. This study established that tailoring the concentration of BSA and pH of the interaction it was possible to reduce aggregation of nanoparticles. Biofunctionalized Ag nanoparticles with reduced aggregation will be more amenable towards bio-sensing applications.

1. Introduction

The size of nanomaterials being similar to that of most biological molecules and structures can be of immense importance for both in vivo and in vitro biomedical research and applications. Biofunctionalization or surface modification is a pertinent technique to obtain biocompatibility in metal nanoparticles for biomedical applications.

One of the major biological functions of albumins is their ability to carry drugs as well as endogenous and exogenous substances [1]. Serum albumins are the most abundant proteins in plasma [2]. As the major soluble protein constituents of the circulatory system, they have many physiological functions [3]. Among the serum albumins, BSA has a wide range of physiological functions involving binding, transport and delivery of fatty acids, porphyrins, bilirubin and steroids, etc. Bovine Serum Albumin (BSA) has been selected as our protein model due to its water-soluble nature which is important for interaction studies [4,5]. It contains 582 amino acid residues with a molecular weight of 69,000, and two tryptophan moieties at positions 134 and 212 as well as tyrosine and phenylalanine [6].

Silver nanoparticles have been known for excellent optoelectronic properties [7–12]. As one of most popular surface enhancement Raman scattering (SERS) active substrates, silver nanoparticles have been used to obtain million fold enhancement in Raman scattering, which provides a high sensitive tool for trace analysis, and even for probing single molecules [7–9]. Coupled with silver nanoparticles, the gold nanoparticle probes have been used to analyze the combinatorial DNA arrays, and both its selectivity and sensitivity exceed those of the fluorescence method [10]. In addition, the silver nanoparticle staining is a sensitive method to determine proteins [11,12]. These studies have exhibited the potential applications of silver nanoparticles.

In absence of extensive prior reports, the interaction mechanisms and especially nanoscale effects about nanoparticles and bio-macromolecules is yet to be well understood, and more so for silver nanoparticles and serum albumins. The major objective of

* Corresponding author. Tel.: +91 416 2202620.
E-mail addresses: amit.mookerjea@gmail.com, amitav@vit.ac.in (A. Mukherjee).

0927-7765/$ – see front matter © 2009 Elsevier B.V. All rights reserved.
doi:10.1016/j.colsurfb.2009.10.005

the present study was to investigate the interaction between silver nanoparticles and the model protein Bovine Serum Albumin in certain concentration range; or precisely the adsorption behavior of BSA over the Ag nanoparticles.

2. Experimental

2.1. Materials

Silver nanoparticles were procured from Sigma Aldrich, USA. The physicochemical parameters as reported by the supplier were: size <100 nm, 99.5% purity, surface area 5 m^2/g and density 10^{-4} g/cc. The dispersions of Ag nanoparticles in Millipore water at 50 ppm concentration were freshly prepared by ultrasonic vibration (100 W, 30 kHz) for 30 min for the interaction studies.

Bovine Serum Albumin (BSA, MW 66 kDa) was purchased from Sigma (A-7030) and the necessary dilutions were made from the stock with nano pure water.

2.2. Characterization of as procured nanoparticles

The aqueous dispersion of the particles was subjected to particle size analysis, by 90Plus Particle Size Analyzer (Brookhaven Instruments Corporation Holtsville, NY, USA). The morphological features of the procured nanoparticles were characterized by Scanning Electron Microscopy (FEI Sirion, Eindhoven, Netherlands). The surface area was measured using a Smart Sorb 93 Single point BET surface area analyzer (Smart Instruments Co. Pvt. Ltd., Mumbai, India). The received particles were also subjected to X-ray diffraction analysis using a JEOL – JDX 8030 diffractometer. The target was Cu K_α ($\lambda = 1.54$ Å). The generator was operated as 45 kV and with a 30 mA current. The scanning range (2θ) was selected from 10° to 100°.

2.3. Adsorption isotherm studies

For adsorption studies of BSA with silver nanoparticles different concentrations of BSA (0.05%, 0.15%, 0.25%, 0.35%, 0.45%, 0.55%, 0.75% and 0.85%) were interacted with silver nanoparticles at a fixed concentration (50 ppm) for 4 h in a rotary shaker at 300 rpm. The interaction was followed by centrifuging at 8000 × *g* for 10 min. The supernatant was carefully collected and the absorbance was recorded in a spectrophotometer (Shimadzu UV-1700, Japan) at 280 nm to measure unreacted BSA concentrations.

To monitor the effect of pH of the medium, the adsorption tests were conducted at pH values 7, 10, and 12 respectively. The uncoated naked nanoparticles were also subjected to pH changes in the dispersion for sake of comparison. The pH buffers for the above mentioned pH were prepared separately using sodium carbonate, sodium bi carbonate (pH 10), disodium hydrogen phosphate and sodium hydroxide (pH 12) and added to the test solutions with different concentrations of BSA and a fixed concentration of Ag nanoparticles. The samples were allowed to interact for 4 h in a rotary shaker at 300 rpm and the absorbance and the peak shifts were recorded in a spectrophotometer (Shimadzu UV-1700, Japan) at a wavelength range of 200–600 nm.

All the tests were carried out in triplicate, and mean values of the results were reported. The experimental error limit was strictly kept within ±5%.

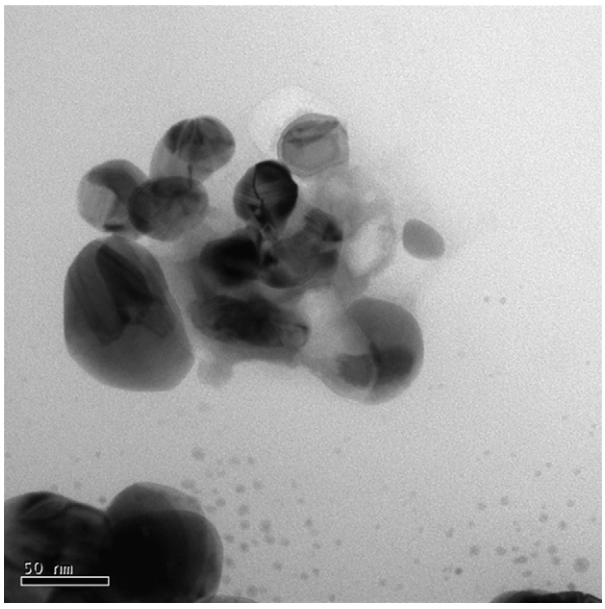

Fig. 1. Transmission electron micrograph of as received Ag nanoparticles uninteracted with BSA.

2.4. UV–vis spectral study

Noble metal silver (Ag) nanoparticles exhibit unique and tunable optical properties on account of their surface plasmon resonance (SPR) dependent on shape, size and size distribution of the nanoparticles. UV–vis spectra of Ag nanoparticle (50 ppm dispersion) and

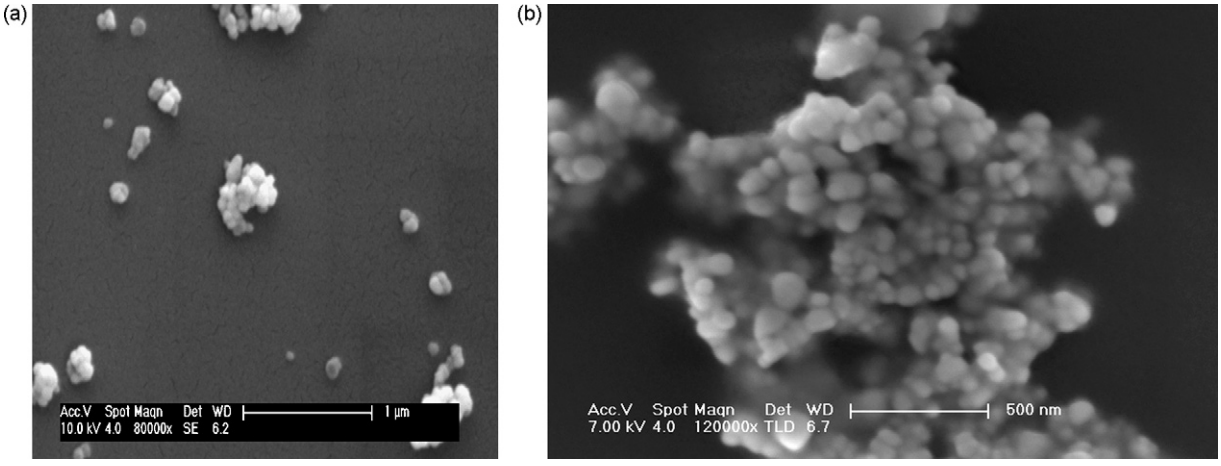

Fig. 2. (a) Scanning electron micrograph of as received Ag nanoparticles uninteracted with BSA. (b) Scanning electron micrograph of BSA coated silver nanoparticles (0.85% BSA with 50 ppm Ag) at pH 7.

BSA mixtures having varying concentrations of BSA were recorded in the UV–vis spectrophotometer (Shimadzu UV-1700, Japan). The investigated spectral range was 200–600 nm. The peak wavelength of the uninteracted silver nanoparticle was found to be 425 nm.

2.5. Morphological and structural studies after adsorption

Morphological features of Ag nanoparticles after interaction with 0.85% BSA were studied using Scanning electron microscope, and high resolution Transmission electron microscope as described in Section 2.2.

The samples were then centrifuged at 11,200 × *g* (10,000 rpm). The pellet was collected, freeze-dried and lyophilized in a Lyophilizer (Thermo Electron Corporation—Micro Modulyo 230 freeze dryer) to get purified powder. The purified powders obtained after 4 h interaction with 0.85% BSA were also subjected to X-ray diffraction analysis as described in Section 2.2.

The purified powder was subjected to FT-IR spectroscopy. These measurements were carried out on a PerkinElmer Spectrum-One instrument in the diffuse reflectance mode at a resolution of 4 cm^{-1} in KBr pellets.

3. Results

3.1. Characterization of as received Ag nanoparticles

The effective diameter of the procured nanoparticles was determined to be 123.5 nm while the ploydispersity was found to be 0.265. The surface area was determined to be 0.26 m^2/g. The TEM image of the as received nanoparticle is shown in Fig. 1. Nearly spherical to elliptical nanoparticles can be observed in the figure. Fig. 2(a) shows the scanning electron micrograph of the as received nanoparticles.

3.2. Morphological studies after interaction

Fig. 2(b) depicts the scanning electron micrograph of the BSA interacted nanoparticles when 0.85% BSA solution was interacted with 50 ppm Ag nanoparticle dispersion at pH 7. From this figure the average size of the each particle in the flock seems to be around 100 nm.

3.3. UV–vis spectral study

The λ_{max} value for uninteracted silver nanoparticle dispersion (50 ppm) was noted at 425 nm. A decrease in absorbance at 425 nm was observed for lower concentrations of BSA, 0.05%, 0.15%, 0.25%, 0.35% (Fig. 3(a)) in absence of noticeable plasmon shift. A blue shift (towards lower wavelength) in λ_{max} value by 5–10 nm was observed beyond 0.45% BSA concentrations. The lowest λ_{max} value was noted at 410 nm.

Fig. 3(b) shows the absorption peaks in range of 250–300 nm. The peak around 280 nm is caused by the $\pi \rightarrow \pi^*$ transition of aromatic amino acid residues [13].

Fig. 4 shows the absorbance decrease for increasing concentration ratios of BSA and Ag nanoparticles (0.05–0.85% BSA to 50 ppm Ag) at λ value of 425 nm. Two distinct modes of relation (two different slopes) between ΔA and [BSA]/[Ag] was clearly noted from the figure indicating stepped adsorption phenomenon. The flat slope in the initial stage of adsorption was noticeable from the Fig. 4.

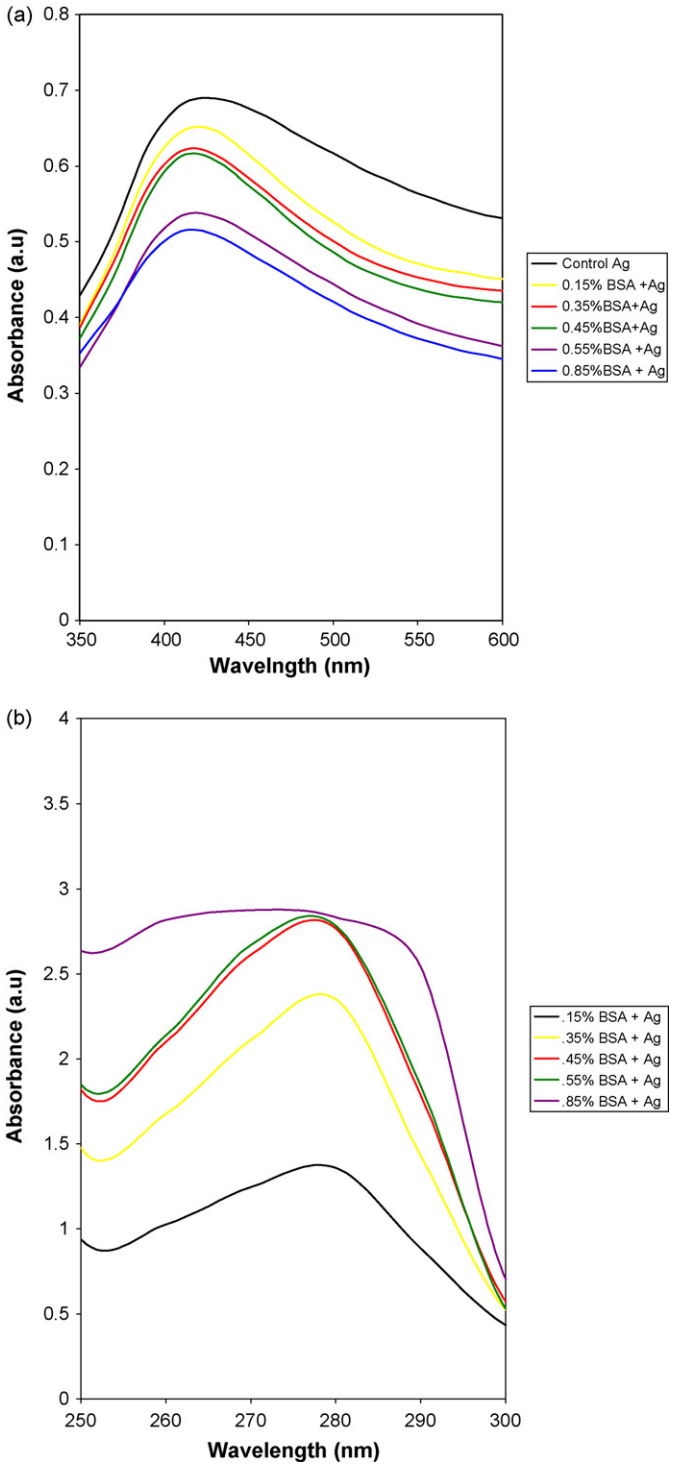

Fig. 3. (a) UV–vis spectra recorded in the range of 350–600 nm as a function of interaction of different concentrations of BSA (0.15%, 0.35%, 0.45%, 0.55%, 0.85%) with Ag nanoparticles (50 ppm) for 4 h. (b) UV–vis spectra recorded in the range of 250–300 nm as a function of interaction of different concentrations of BSA (0.15%, 0.35%, 0.45%, 0.55%, 0.85%) with silver nanoparticles (50 ppm) for 4 h.

3.4. Adsorption isotherms

The search for best-fit equation using the linear regression analysis was the most commonly used technique to determine the best-fit isotherm and the method of least squares has been used for finding the parameters of the isotherm. The adsorption data were fitted to linearized forms of both Langmuir and Freundlich isotherms to find out the optimum isotherm relationship. In our case BSA and silver nanoparticles were the adsorbate and adsorbent respectively. Thus, the isotherms are plotted as a function of

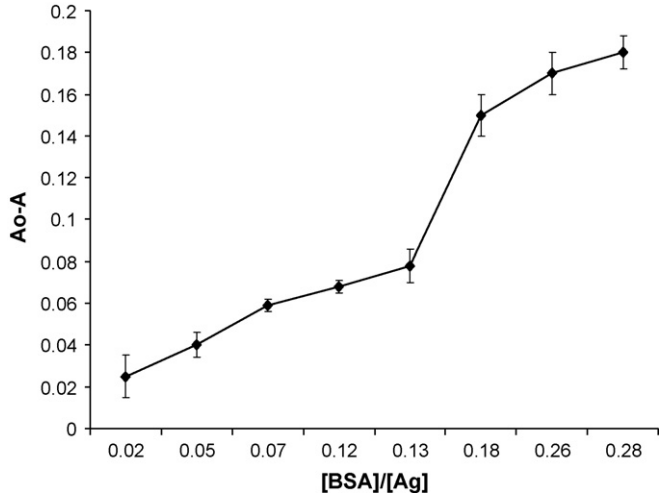

Fig. 4. The plot of mean values of A_o–A vs [BSA]/[Ag] where A_o is the absorbance value of the plasmon band of silver nanoparticles and A is the absorbance values of silver nanoparticles interacting with BSA. The mean values were calculated and the error bars have been plotted in the graph.

BSA/Ag and Equilibrium concentration of BSA.

Equation for Freundlich isotherm is : $q_e = K_f \cdot C_e^{1/n_f}$ (Ia)

Linear form of Freundlich isotherm is : $\log q_e = \frac{1}{n_f} \log C_e + \log k_f$ (Ib)

Equation for Langmuir isotherm is : $q_e = \frac{(q_m K_a C_e)}{1 + K_a C_e}$ (IIa)

Linear form of Langmuir isotherm is : $\frac{C_e}{q_e} = \frac{C_e}{q_m} + \frac{1}{K_a q_m}$ (IIb)

where, C_e (mg/l) is the amount of adsorbate in solution at equilibrium; q_e (mg/mg) is the amount of adsorbate adsorbed per gm of adsorbent; n_f, k_f, K_a, q_m are constant.

Fig. 5(a) and (b) show adsorption data plotted following Eqs. (Ib) and (IIb) respectively. The Freundlich parameters obtained from the Fig. 5(a) were: $n_f = 0.919$, and $k_f = 0.717$ respectively. The Freundlich isotherm constants were also manually calculated solving the simultaneous equations as shown in Table 1. In both the cases the constants were found to be approximately same. In linearized form of Langmuir the constants found were: $q_m = -476.19$ and $K_a = 0.0019$. The Langmuir isotherm constants were also manually calculated, the value were determined to be $q_m = 130.25$ and $K_a = 0.0073$. The large variations between the graphical solution, and analytical solutions indicated that the experimental data did fit well in Langmuir form. It was also observed comparing the Fig. 5(a) and (b) that adsorption data fitted

Table 1
The analytically calculated Freundlich isotherm constants (n_f, k_f) at different concentrations of BSA (by solving simultaneous equations).

Concentration	q_e	C_e	$\log q_e$	$\log C_e$	n_f	k_f
0.05%	9.78	11.1	0.99	1.045	0.88	0.64
0.15%	29.4	29.27	1.468	1.466	0.88	0.63
0.25%	49	48.3	1.69	1.684	0.91	0.73
0.35%	68.68	65.8	1.836	1.818	0.91	0.69
0.45%	88.6	103	1.947	1.929	0.94	0.80
0.55%	108	102.4	2.033	2.010	0.94	0.79
0.75%	148	122.4	2.178	2.087	0.92	0.73
0.85%	168	137.6	2.225	2.1386	0.92	0.83

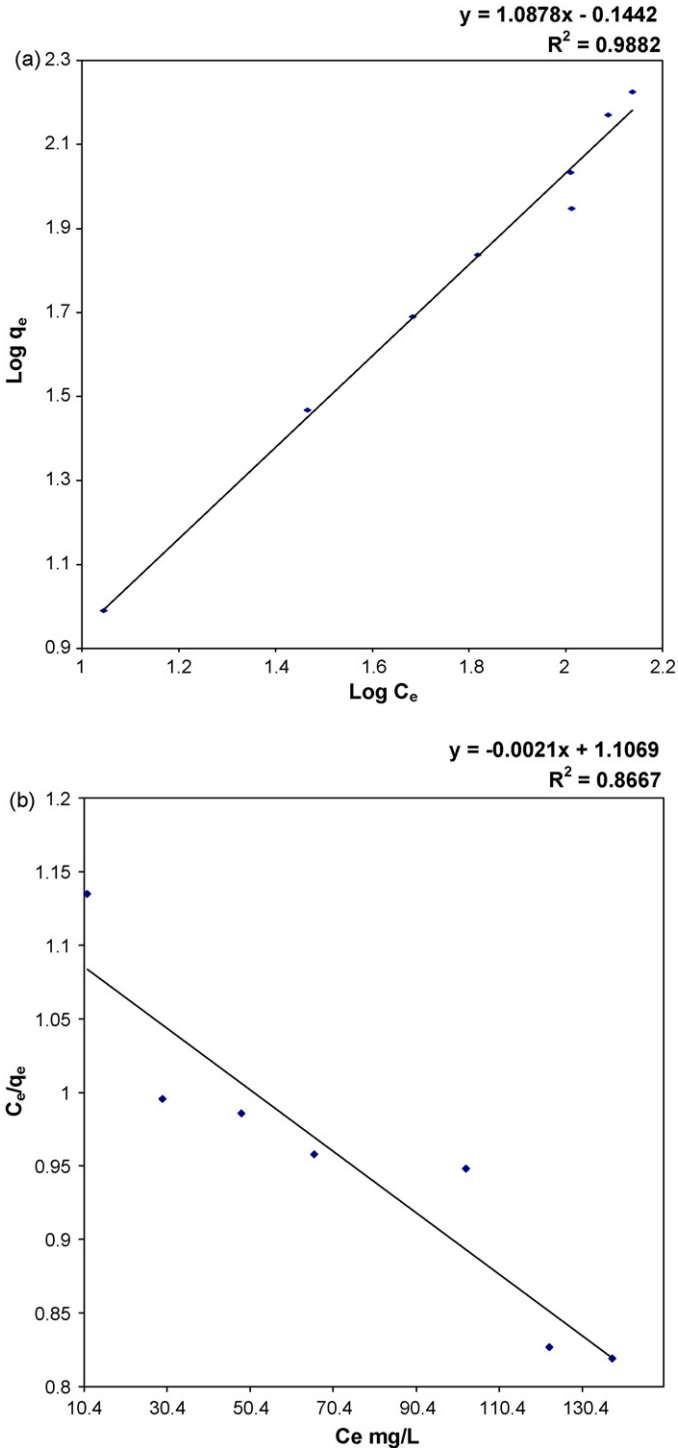

Fig. 5. (a) The Freundlich isotherm plotted as a function of $\log q_e$ vs $\log C_e$ for different concentrations of BSA interacted for 4 h with silver nanoparticles (50 ppm), where C_e (mg/l) is the amount of adsorbate in solution at equilibrium and q_e is the amount of BSA (mg) adsorbed per mg of silver nanoparticles. (b) The Langmuir isotherm plotted as a function of C_e/q_e vs C_e for different concentrations of BSA interacted for 4 h with silver nanoparticles (50 ppm), where C_e (mg/l) is the amount of BSA in solution at equilibrium and q_e is the amount of BSA adsorbed per mg of silver nanoparticles.

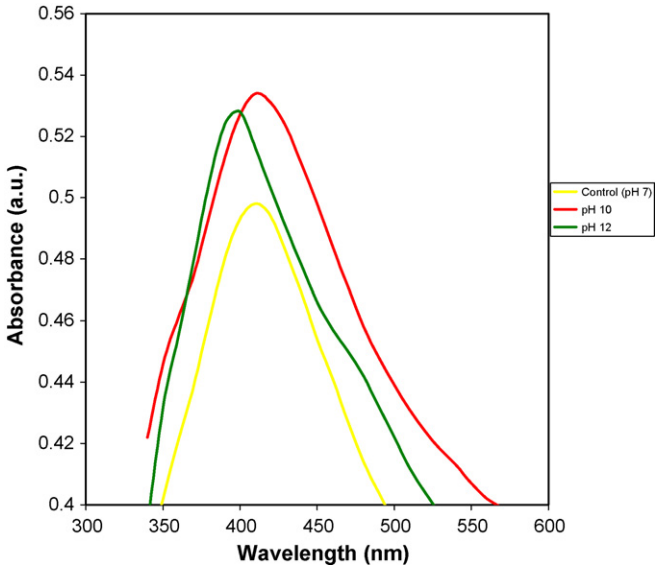

Fig. 6. UV–vis spectra of BSA coated silver nanoparticles (0.85% BSA with 50 ppm Ag) recorded as a function of pH.

better to linear Freundlich isotherm ($R^2 = 0.988$) than to Langmuir ($R^2 = 0.866$).

3.5. Effect of increase in pH of the medium

Fig. 6 shows the effect of varying pH on interaction of Ag nanoparticles with 0.85% BSA. At pH 7, and 10 the λ_{max} value was noted at 410 nm, unchanged from the control test results. At highly alkaline pH 12, the plasmon band shifted to 400 nm. The uncoated Ag nanoparticles however did not show noticeable plasmon shift at these pH values. Moreover it was found that the pH buffers did not interfere with the experimental results.

3.6. FT-IR spectroscopy and XRD pattern of the interacted Ag nanoparticles

The interacted silver nanoparticles (0.85% BSA, 50 ppm Ag) at pH 7 were subjected to FT-IR spectroscopy to monitor the structural conformations (if any) owing to interactions (Fig. 7).

The XRD pattern did not show any characteristic peak of Ag nanoparticles which clearly shows that the metal nanoparticle has been completely coated with BSA (figure not shown).

4. Discussion

The localized surface plasmon resonances are collective oscillations of the conduction electrons confined to metallic nanoparticles. Excitation of the localized surface plasmons causes strong light scattering, by an electric field at a wavelength where resonance occurs; this phenomenon results in appearance of strong surface plasmon absorbance (SPR) bands. The optical absorption spectrum of metal nanoparticles is dominated by the SPR which exhibits a shift towards the red end or blue end depending upon the particle size, shape, state of aggregation and the surrounding dielectric medium [14]. For silver nanoparticles of λ_{max} values were reported in the visible range 400–500 nm [15]. In this study the plasmon band of the uninteracted Ag nanoparticles was noted at 425 nm.

The isoelectric point of BSA is between 4.5 and 4.9 [16]. Since the reaction pH for the interaction studies was above the isoelectric point, the BSA molecules had a significant number of negatively charged functional groups attached on the surface, which formed the attractive coulombic interaction between the protein and the silver nanoparticles. The charged functional groups can be considered weak neucleophile, but nucleophilic enough to bind the metal particles. In the initial mode of spectral change with increasing [BSA]/[Ag] ratio the anionic functional groups were strongly adsorbed onto the silver particles, the ΔA (decrease in absorbance) was sharp [Fig. 4] the plasmon band decreased in intensity and broadened without shift in λ_{max} value (425 nm), which may be attributed to less availability of excess electrons on the surface owing to strong chemisorption. The two different slopes for ΔA – [BSA]/[AgNP] curves indicated stepped formation of adsorption layers of BSA on metal surface [17]. Two possible mechanisms of BSA binding to nanoparticles have been suggested: either "end on" or "side-on" binding, in which end-on binding results in a higher surface coverage of BSA on the surface. Proteins can be attached to the surface by chemical cross-linking reagents, or they can spontaneously assemble because of the electrostatic forces. In the layer-by-layer approach, the binding of a protein to the surface of a colloid is achieved by electrostatic interactions. [18].

Assuming change in absorbance (ΔA) with [BSA]/[AgNP] can be directly correlated to the absorption behavior of BSA on the particles, in the initial stages adsorption was not very rapid (a flat slope), which corroborated to non Langmuirian adsorption behavior. Expectedly the equilibrium data fitted better to Freundlich isotherm.

On further increasing the concentrations of BSA, Ag colloids with adsorbed layers of BSA started repelling each other. This increased electrostatic repulsion enhanced stabilization of the colloids preventing flocculation. The breaking up of the agglomerates/flocs (reversible flocculation) would result in a blue shift due to size dependent phenomenon [15]. According to another explanation, with increasing BSA concentration, surface charge density on the Ag colloids would increase. The negatively charged surface functional groups will then restrict the free electrons of the Ag colloids within a smaller volume leading to an increased free electron density, thus a higher plasmon frequency (lower wavelength) [19]. This might have triggered the blue shift at beyond 0.45% BSA concentrations.

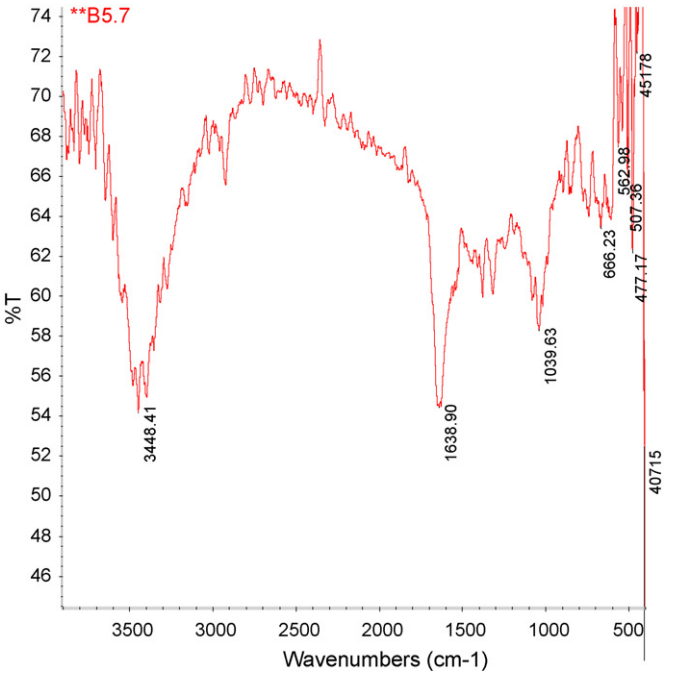

Fig. 7. FT-IR spectra of BSA coated silver nanoparticles (0.85% BSA with 50 ppm Ag nanoparticles) at pH 7.

With increasing pH of the medium to pH 12, there was a further blue shift in plasmon band to 400 nm, which might be contributed to enhanced negative charge on BSA, which in turn induced additional surface charge on the Ag nanoparticles, increasing the free electron density further.

In another viewpoint the denaturation of BSA at highly alkaline pH values caused multilayer of protein interacting strongly with the nanoparticle surface through hydrophobic groups. The changes in UV absorption peaks in 250–300 nm may be attributed to the conformational changes of BSA upon interaction with Ag nanoparticles in basic pH ranges, which caused the gradual perturbation of the microenvironments around aromatic amino acid residues, and resulted in the gradual exposure of the residues such as tryptophan (Trp) and tyrosine (Tyr) inside the hydrophobic cavities [17]. The indole nitrogen of Trp and the phenolate oxygen of Tyr residues could be deprotonated in alkaline systems, which facilitates the adsorption onto the surface of positively charged silver nanoparticles.

The X-ray diffraction study corroborated with adsorption of BSA on nanoparticles surface, the coverage was so strong no characteristic band of silver could be revealed through XRD. The SEM micrograph after interaction with BSA demonstrated that shape of the nanoparticle did not suffer distinct modifications. The average size range also remained around 100 nm proving the anti-aggregation behavior of BSA coating.

Amide I and Amide II are the most important bands of the protein infra red spectrum [20]. In free BSA the Amide A band was obtained at about 3500 cm^{-1} and an Amide I band obtained between 1600 and 1700 cm^{-1} [21]. Amide A is more than 95% in proteins and is mainly due to N–H stretching vibration. Absorption in the amide I region is based on C=O stretching vibrations of the amide group weakly coupled to the in-plane N–H bending and C–N stretching modes and is indicative of the presence of interactions leading to the formation of secondary structure elements [22]. Since the FT-IR studies revealed only the structural characteristics of BSA, proving complete coverage of the nanoparticles by BSA.

In a similar study albeit with gold nanoparticles a group of researchers observed that the pH dependent optical properties of the colloids coated with BSA were quite different from the uncoated ones. The BSA coating prevented the gold nanoparticles from aggregating in solutions of pH greater than 5 and, thus, eliminating the time-varying red-shifting peak observed in the spectra of the uncoated gold nanoparticles. There are other reports also stressing that the modification with protein is known to stabilize the Au colloidal solution generating additional repulsion energy term [23,24].

5. Conclusion

In conclusion, the UV–vis absorption spectral properties of silver nanoparticles coated with BSA were observed to be quite different from the uncoated particles. The BSA adsorption on the surface prevented the Ag nanoparticles from aggregating in solutions of pH greater than 5. A noticeable increase in absorbance was noted in the peak range of 250–300 nm, which may be attributed to the conformational changes of BSA upon interaction with Ag nanoparticles. With increasing concentrations of BSA, initially a decrease in intensity of the absorption spectra was noticed without change in plasmon peak. The decrease in absorbance was commensurate with a stepped adsorption layer behavior. Beyond 0.45% BSA concentrations, a blue shift in the plasmon band from 425 to 410 nm was noticed.

Since the results obtained from FT-IR spectroscopy revealed the prominent peaks of proteins, the complete coating of nanoparticles by BSA can be confirmed. The equilibrium adsorption data fitted better to linearized Freundlich isotherm compared to Langmuir curve. The increase in pH to 12 shifted further the plasmon band to 400 nm. BSA itself might have suffered conformational changes in basic pH ranges, causing strong hydrophobic interactions with the nanoparticles.

The aggregation of the silver nanoparticles may prevent the uptake of these nanoparticles in live cells and limit their applicability as bioprobes. Moreover biocompatibility of the particles is one of the pre requisites to bio-sensing applications. This study demonstrates that by tailoring the concentration of BSA and pH of the medium it is possible to reduce aggregation and flocculation effects. Additional studies are needed to determine an optimal thickness for the BSA coating and to establish detailed mechanistic aspects of the process.

Acknowledgements

The authors are grateful to Ms Prathna Chandrasekaran, for X-ray diffraction, SEM, and TEM studies. Ms. Jyoti and Ms. Kainaz are greatly acknowledged for carrying out a few preliminary tests on absorption.

References

[1] F. Moreno, M. Cortijo, J.G. Jimenez, Photochem. Photobiol. 70 (1999) 695.
[2] D.D. Carter, J.X. Ho, Adv. Protein Chem. 45 (1994) 153.
[3] R.E. Olson, D.D. Christ, Ann. Rep. Med. Chem. 31 (1996) 327.
[4] J. Valanciunaite, S. Bagdonas, G. Streckyte, R. Rotomskis, Photochem. Photobiol. Sci. 5 (2006) 381.
[5] U.K. Hansen, Pharmacol. Rev. 33 (1981) 17.
[6] L.A. Sklar, B.S. Hudson, R.D. Simoni, Biochemistry 16 (1977) 5100.
[7] S. Nie, S.R. Emory, Science 275 (1997) 1102.
[8] X.M. Dou, Y.M. Jung, Z.Q. Cao, et al., Appl. Spectrosc. 53 (1999) 1440.
[9] P.C. Lee, D.P. Meisel, J. Phys. Chem. 86 (1982) 3391.
[10] T.A. Taton, C.A. Mirkin, R.L. Letsinger, Science 289 (2000) 175.
[11] M. Moeremans, G. Daneels, De. J. Mey, Anal. Biochem. 145 (1985) 315.
[12] C.Q. Zhou, D.H. Li, Q.Z. Zhu, J. Fresenius, Anal. Chem. 366 (2000) 863.
[13] J. Huang, Y.Z. Yuan, H. Liang, Science in China, Series B 46 (2003) 387.
[14] C. von Fragstein, F.J. Schoenes, Z. Phys. 198 (1967) 477.
[15] N. Mohri, M. Inoue, Y. Arai, K. Yoshikawa, Langmuir 11 (1995) 1612.
[16] C. Chaiyasut, T. Tsuda, Chromatography 22 (91) (2001).
[17] P. Manavalan, W.C. Johnson Jr., Nature 305 (1983) 831.
[18] E.W. Stein, M.J. McShane, IEEE Trans. Nanobiosci. 2 (3) (2003) 133.
[19] T. Siebrands, M. Giersig, P. Mulvaney, C.H. Fischer, Langmuir 9 (1993) 2297.
[20] P. Athina, J.G. Rebecca, A.F. Richard, J. Agric. Food Chem. 53 (2005) 158.
[21] A. Dong, P. Huang, W.S. Caughey, Biochemistry 29 (1990) 3303.
[22] N. Totowa, Methods in Molecular Biology, 22, Humana Press Inc., 1994.
[23] C. Mangeney, F. Ferrage, I. Aujard, et al., J. Am. Chem. Soc. 124 (2002) 5811.
[24] C.S. Weisbecker, M.V. Merritt, G.M. Whitesides, Langmuir 12 (1996) 3763.